Ecological Indicators 71 (2016) 302–316

Contents lists available at ScienceDirect

Ecological Indicators

journal homepage: www.elsevier.com/locate/ecolind

Coastal-flood risk management in central Algarve: Vulnerability and flood risk indices (South Portugal)

A.M. Martínez-Graña[a,*], T. Boski[b], J.L. Goy[a], C. Zazo[c], C.J. Dabrio[d]

[a] Department of Geology, Faculty of Sciences, Square Merced s/n, 37 008 Salamanca, University of Salamanca, Spain
[b] Centre for Marine and Environmental Research CIMA, Edificio 7, Campus Universitário de Gambelas, Universidade Algarve, 8005 Faro, Portugal
[c] National Museum of Natural Sciences, Section Geology, Street José Gutiérrez Abascal n° 2, 28006 Madrid, Spain
[d] Department of Stratigraphy, Faculty of Geology, Complutense University, 28040 Madrid, Spain

ARTICLE INFO

Article history:
Received 3 March 2016
Received in revised form 12 July 2016
Accepted 14 July 2016
Available online 22 July 2016

Keywords:
AVI Index
FRI Index
Flood risk
Vulnerability
Coastal management
GIS

ABSTRACT

This paper presents an analysis of the vulnerability (AVI Index) and hazard of flooding by sea level rise (FRI Index) in the central Algarve (South Portugal), between the cities of Portimão and Tavira, which is an area of intense urban impact and fast growing tourism. The vulnerability index was calculated using the following parametric thematic maps: lithology, geomorphology, slopes, elevations, distances, bathymetry, variations of the coastline, wave height and activity, variations of sea level and tidal range. The AVI Index was validated by the results obtained from the analysis of the risk of flooding from the FHI Index applied to several time horizons (X_0-present, X_1-100 years, X_2-500 years, X_3-1000 year, X_4-Storm and X_5-Tsunami). Application of GIS and remote sensing techniques, viz. spatial analysis, interpolation processes and geostatistical analysis, permitted a regional forecasting model of change in the mean sea level and the ensuing consequences to be established. Analysis of the obtained results shows an increase in potential flood zones in populous coastal tourist areas with a high risk of exposure and a significant spatial extent of 8.84 km^2 only in Faro municipality. The assessment and delineation of other endangered sectors could contribute to designing appropriate long- term management policies for the coastal of Central Algarve.

1. Introduction

The paradigm of "Global change" is a subject that has attracted the attention of the scientific community for decades and became a truly hot topic after the 1982 Rio de Janeiro Earth Summit. Often climate change and global change are equated, and climate and "global warming" are commonly used as an all in one explanation for all sorts of changes or processes currently taking place at the Earth's surface (Zazo, 2015).

According to the latest report by the Intergovernmental Panel on Climate Change (IPCC, 2014), the warming of the climate system is unequivocal. Since 1950 there have been unprecedented changes in the climate systems, which can be seen in both the observational historical records, from the late nineteenth century, and with paleoclimatic records spanning the last millennia. These changes are manifested, by the warming of the atmosphere and oceans, decrease in the mass of cryosphere, and by an increase in the concentrations of atmospheric greenhouse gases, among other types of processes.

Global studies of the current sea level indicate a sustained rise that has occurred since the late nineteenth century, with a turnaround and acceleration in the second half of the twentieth century. This trend can be seen in tide gauge records since 1880, and has been largely confirmed by the sea surface elevation data recorded by several altimetric satellite missions: Topex-Poseidon, Jason I, and OSTM-Jason II (Tooley and Jelgersma, 1992; Church and White, 2011). The available figures obtained from the tide gauges point to a rate of increase around of 2.8 ± 0.8 mm/year, whereas values provided by satellite missions amount to 3.2 ± 0.4 mm/year (Church et al., 2013).

The physical phenomena behind the rise of the global average sea level are primarily ocean thermal expansion and the melting of glaciers. Tectonics and salinity only have a local influence (Table 1).

There is a wide variability in projections of future sea level rise, which have been estimated as: 21–48 cm (Meehl, 2007), 50–135 cm (Bindoff et al., 2007; Rahmstorf, 2007), 60–115 cm (Vellinga and

* Corresponding author.
E-mail addresses: amgranna@usal.es (A.M. Martínez-Graña), tboski@ualg.pt (T. Boski), joselgoy@usal.es (J.L. Goy), mcnzc65@mncn.csic.es (C. Zazo), dabrio@ucm.es (C.J. Dabrio).

http://dx.doi.org/10.1016/j.ecolind.2016.07.021
1470-160X/

Table 1
Contributions to the balance of sea level since 1972 (Church et al., 2013).

Components	1972–2008 (mm/year)	1993–2008 (mm/year)
Tide-gauge (Total)	1.83 ± 0.18	2.61 ± 0.55
Tide-gauge and altimeter (Total)	2.10 ± 0.16	3.22 ± 0.41
1. Thermal expansion	0.80 ± 0.15	0.88 ± 0.33
2. Glaciers and ice sheets	0.67 ± 0.03	0.99 ± 0.04
3. Ice of Greenland	0.12 ± 0.17	0.31 ± 0.17
4. Antarctic ice	0.30 ± 0.20	0.43 ± 0.20
5. Terrestrial storage	−0.11 ± 0.19	−0.08 ± 0.19
Sum of components (1+2+3+4+5)	1.78 ± 0.36	2.54 ± 0.46

Wood, 2008), 85–200 cm (Pfeffer et al., 2008), 60–95 cm (Kopp et al., 2009), 80–190 cm (Vermeer and Rahmstorf, 2009), 78–160 cm (Grinsted et al., 2010), >100 cm (Katsman and Oldenborgh, 2011) for the XXI Century During the period 1901–2010, the global mean sea level raised an average of 1.7 [1.5–1.9] mm/year, a rate higher than that of the previous two millennia (Church et al., 2013).

The projections of the change in sea level at a regional scale, suggest that it is very likely that in the XXI century and later, changing sea levels will have a pronounced regional pattern, with significant deviations from the global average. In the Fifth Assessment Report (Conde, 2015; Church et al., 2013; IPCC, 2014), it is postulated that during decadal periods, these regional variation rates resulting from climate variability, may differ by more than 100% from the global average.

There is growing public awareness of the impacts that climatically driven environmental changes may have on the socio-economic sphere. For instance, The European Union's directive 2007/60/EC (DOUE 60, 2007) was promulgated due to the increased frequency of catastrophic events—213 major flooding events with 1126 deaths and the loss of 52 billion Euros (Jonkman and Kelman, 2005). Currently, there is a need for a renewed assessment policy and flood risk control measures in all of the member states, both in coastal and inland Settings. To manage the risk offloods, a detailed analysis of the variables affecting the current sea level rise is required in order to develop a reliable simulation model, and mapping (Kurt et al., 2004, 2011; Kulkarni et al., 2014). Such mapping is, a very effective tool, that is widely used in planning and environmentally-oriented land management.

The Algarve coastline is vulnerable to sea level rise, and in particular along beaches, deltas, tidal flats and coastal wetlands. Human activity in these areas, especially tourism, brings about additional challenges in terms of increasing vulnerability and degree of exposure to the hazard. Therefore a study involving short and medium-term flood risk is most needed. Widespread flooding of Albufeira in November 2015, during the torrential precipitation associated to a storm surge was reported to have caused material losses in excess of 10M euro, and is a clear example of the need for prevention plants. Likewise, estimating the possible rise in sea level, whatever the timescale, may prevent or, at least, induce protection and mitigation measures, both in structural and land use planning terms, aimed to minimize the presumable social impacts involved. It is estimated that, worldwide, some 200 million people live in coastal areas, a figure expected to rise up to 600 million in 2100 (Nicholls and Mimura, 1998).

The objectives of this study were to assess the degree of vulnerability to changes in sea level and the risk of flooding in the coastal sector between Portimão and Faro in central Algarve (South Portugal) (Fig. 1). The study area, includes two clearly differentiated sectors: to the east the Ria Formosa tidal flats laying behind the protecting sandy spits and barrier islands that migrated under an eastward-moving longshore drift (Andrade et al., 2004); and to the west, the mostly rugged coastline extending between the cities of Portimão and Albufeira, with beaches and urban areas protected by rocky outcrops.

Vulnerability was calculated using empirical methods that combined a series of integrated factors from parametric maps, from the Algarve vulnerability index –AVI-created by the authors based on Ojeda et al. (2009) changing some parameters for the Algarve area using GIS (ArcGis v10.3). For the purpose of the flood risk analysis deterministic methods were used by assigning a probability of sea level rise based on a variety of foreseeable temporal scenarios (100 years, 500 years, 1000 years, storms and tsunamis).

2. Material and methods

2.1. Vulnerability analysis for coastal flooding

The vulnerability was assessed by means of the Algarve vulnerability index—AVI-, similar to that used by the US Geological Survey (Hammar-Klose and Thieler, 2001) applied to the American Atlantic coast, Pacific and Gulf of Mexico, and also validated in the Spanish Andalusian coast near the area of the present study (Ojeda et al., 2009). This index was adapted and modified according to the intrinsic parameters of the study area, considering ten factors that made up the index AVI equation (Eq. (1)) and are explained below:

$$AVI = \sqrt{Fl \times Fg \times Fs \times Fh \times Fd \times Fb \times Fc \times Fw \times Fsl \times Ftr/10} \quad (1)$$

2.1.1. Lithologic factor (Fl)

This factor created a parameter which indicated the resistance of rock units against marine erosion.

From a geological point of view, two different areas (Manuppella et al., 2007) are recognized along the Algarve coastal fringe: a northern area with carbonate Mesozoic formations and a southern one, where diversely consolidated detrital sediments of Cenozoic age predominate. These terrains are easily and immediately differentiated by their topographic relief. The oldest materials correspond to the Late Triassic evaporitic marls that evolved into salt diapirs under the cities of Faro and Loulé. During the Jurassic period, fossiliferous carbonate formations with abundant marine fossils were deposited, with an erosional event in the Middle Jurassic. Cretaceous carbonates lay unconformably on top. N-S faults promoted tilting of blocks. During the Miocene, biocalcarenites (Pais et al., 2012) with abundant marine fossils and sandstones with interbedded glauconitic silts accumulated, heavily deformed by the undergoing diapirism. Five Plio-Pleistocene (Moura and Boski, 1999; Moura et al., 2009) fluvial to marine units accumulated on a karstified surface of Miocene age (Pereira and Cabral, 2002). In ascending stratigraphic order, these are: Falesia feldspathic sands, Montenegro burrowed sands of Montenegro, Quarteira orange sands, Ludo yellow sands, and Gambelas pebbly sands. There are also gravel terraces and fluvial channel-fills of Pleistocene age covering Jurassic limestones. Finally during the recent Holocene, coastal sands accumulated as beaches and dune systems, barrier islands, and silts as tidal flats and tidal marshes of the sheltered channels of Ria Formosa. Terrestrial deposits accumulated in alluvial river channel, flood plains and low terraces.

For the analysis of the lithological factor, the geological materials are grouped into five classes according to the "hardness" against a possible arrival of the sheet of water. Then, the most recent unconsolidated materials (grain sand, gravel, etc.) have less resistance to the effect of the water surface meaning sectors more vulnerable to an advance of the sea than the most consolidated lithologies: basalts (value 1), limestones and marls (value 2), are more resistant to ascending sea level than biocalcarenites and sandstones (value 3), conglomerates, clays and silts (value 4) and sand and gravel (value 5) (Fig. 2).

Fig 1. Location of the study area within the Gulf of Cadiz and main localities.

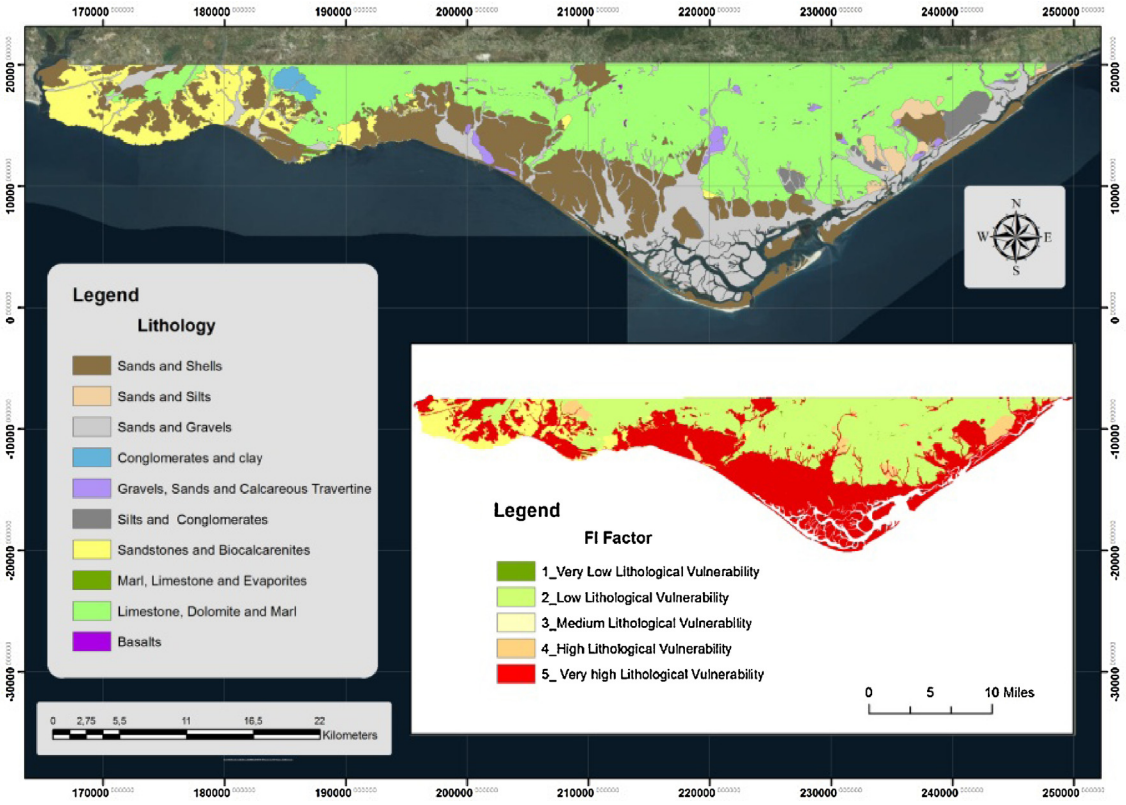

Fig. 2. Lithological map (based on Manuppella et al., 2007) and vulnerability map after lithologic reclassification.

2.1.2. Geomorphic factor (Fg)

We distinguished three major units: mountainous terrain, liaison units and those resulting from the greater or lesser activity of coastal dynamics. The mountainous terrain include the mountains and hills carved in Paleozoic and Mesozoic carbonates, grewacke, shale and basalt to the north which are the main source areas of sediment. External geodynamic agents are responsible for dismantling, giving rise to various geomorphological formations, such as alluvial fans, glacis, endorheic areas, which constitute the liaison units between the mountains and hills and the coastal environments. The coastal unit consists of spit bars, beaches, dune systems, offshore shelf, cliffs, marshes, etc. Beaches and dune systems occupy a significant part of the spit that forms the barrier island where the building boom has destabilized the erosion/sedimentation balance,

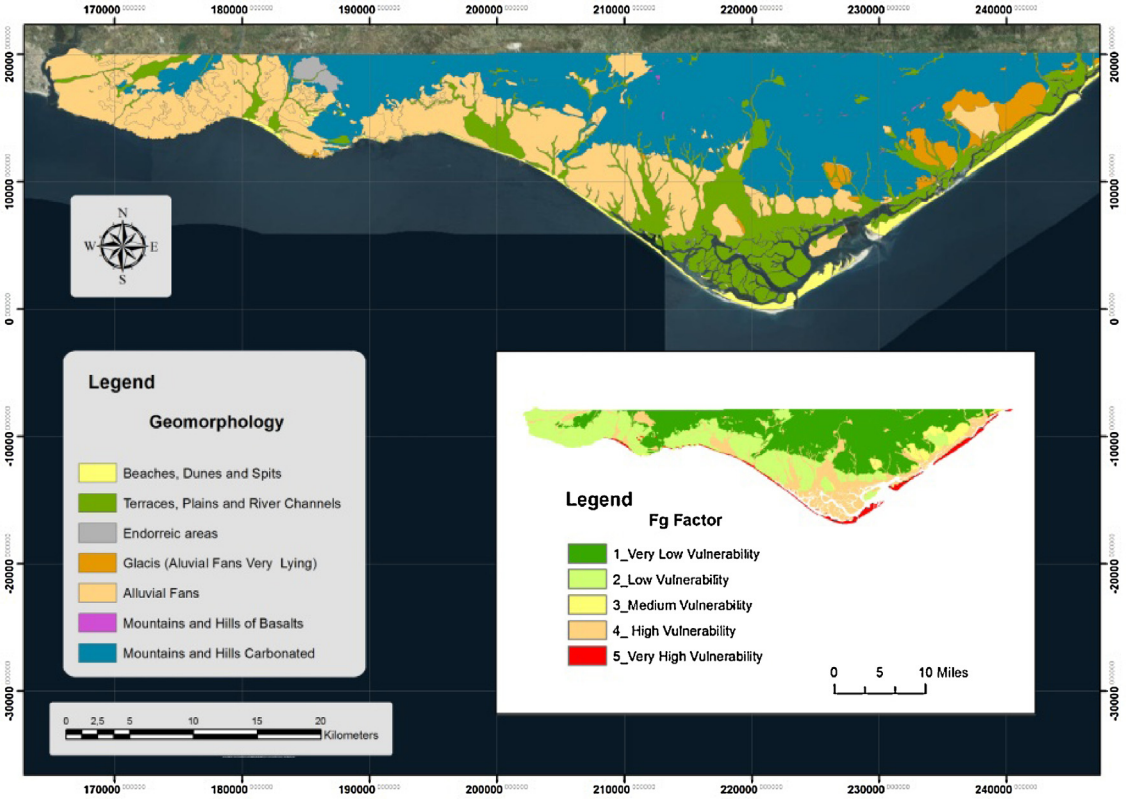

Fig. 3. Geomorphological mapping and vulnerability reclassification.

causing a loss of sand in coastal fronts (Moura et al., 2006; Rodrigues et al., 2012). The spatial distribution of the geomorphological units and associated surface formations, allows establishing degrees of resistance according to future stage location under the sea surface, showing the degree of disaggregation of each formation. We assigned vulnerability values from 1 to 5, where 1 means very low vulnerability and 5 means very high vulnerability. According to this, we assigned a value 1 to mountains and hills, 2 to alluvial fans, 3 to glacis, 4 to fluvial and marine terraces and endorheic areas, and 5 to all coastal sedimentary environments: beaches, dunes, spits and channels (Fig. 3).

2.1.3. Slope factor (Fs)

The slope of the ground largely influences the inundation during a rise of sea level either sporadic (tsunamis and storms) or permanent. Inclination also controls the velocity of withdrawal of sea water faced to a potential flooding by inland waters. Lower slopes increase the rate of displacement of the shoreline towards the sea (Pilkey and Davis, 1987).

To produce parametric maps of slopes, we generated a Digital Terrain Model—DTM-, in which each pixel has the value of the height (Digital Elevation Model), joining the lidar model of year 2011 (coastal strip 150 m from the coastline inland) where spatial resolution is 2 m, and the continental Digital Terrain Model of year 2013, where resolution is 25 m. This produces a map of slopes expressed in percentages, interpolating with a spatial resolution of 1 m, by weighting the vulnerability, taking into account that lower slopes are more vulnerable because penetration of sea water is easier. The map shows 5 intervals: 0–1% (value 5), 1–2% (value 4), 2–4% (value 3), 4–6% (value 2) and >6% (value 1) (Fig. 4).

2.1.4. Height factor (Fh)

The height factor is one of the most important when assessing the current risks related to a rise of sea level. We consider the limit at 10 m, a height considered unattainable under the current estimations of potential sea level rise in the next 100 years (IPCC, 2014). Areas with elevation above 10 m are assigned low levels of vulnerability, in contrast with areas close to elevation 0 m, particularly if laterally related to the shore, with maximum levels of vulnerability assigned to the coastal fronts of barrier islands, estuaries and beaches. Vulnerability decreases gradually when moving inland. We have considered the 10 m high to analyze the entire coastline including more distant land of the coastline. Values of vulnerability were reclassified using the values of elevation in the DTM. The height values for each pixel are: 0–2 m (value 5), 2–4 m (value 4), 4–6 m (value 3) 6–10 m (value 2) and >10 m (value 1) (Fig. 5).

2.1.5. Distance factor (Fd)

Closely related to height and slope factors, the distance factor considers the linear distance between the present coastline and a hypothetical coastline placed at elevation 10 m, whose contour was derived from digital processing of the DTM. The distance factor estimates the capacity of rising sea water to advance inland from the present Algarve coast, provided that there is spatial continuity with the sea. This parameter was calculated using an extension for ArcGIS created by the American USGS "Digital Shoreline Analysis System"—DSAS-. With this tool, we calculated the linear distances between the 10 m contour with respect to the 2014 coastline. Distances were checked by means of nested vector buffer validating techniques, and a raster layer was generated whose data have been reclassified based on the standard deviation, with intervals 0–700 m (value 5), 700–3000 m (value 4), 3000–5000 m (value 3), 5000–9000 m (value 2) and >9000 m (value 1) (Fig. 6).

2.1.6. Bathymetry factor (Fb)

Knowledge of the continental shelf gives invaluable information for understanding the action of waves. As waves approach the coast, their shape changes once the water depth is smaller than half the

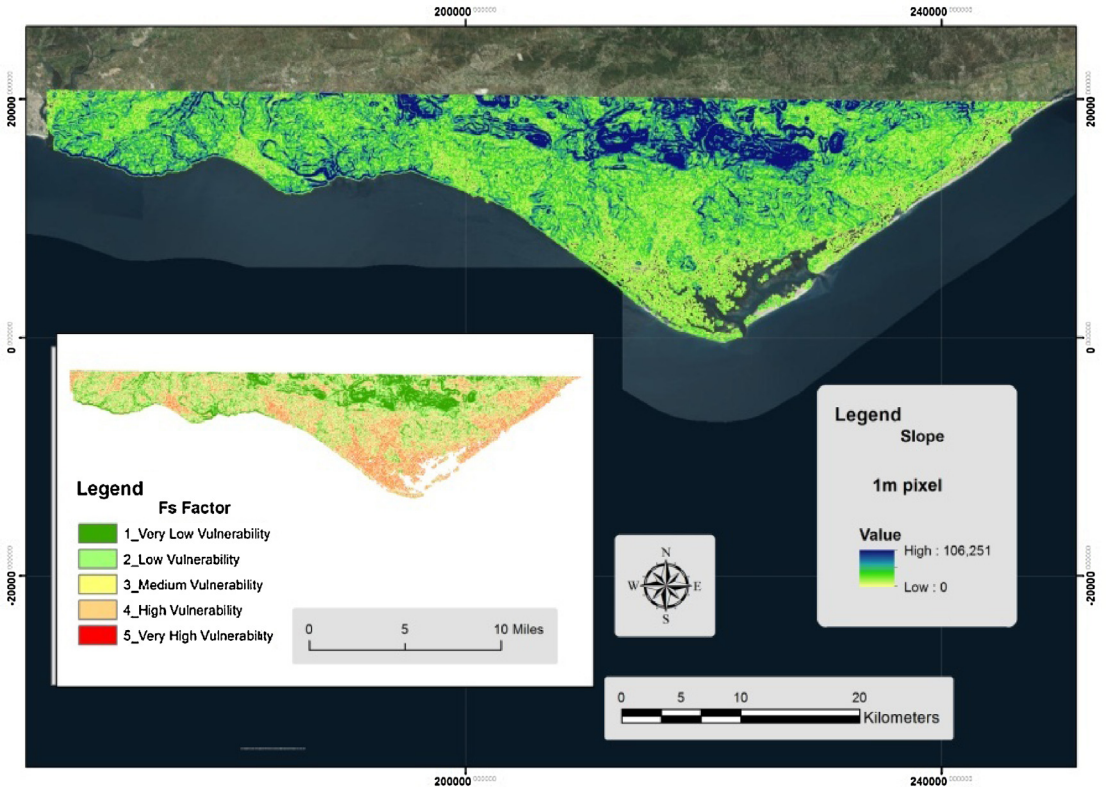

Fig. 4. Slope map (in%) and reclassification in terms of vulnerability.

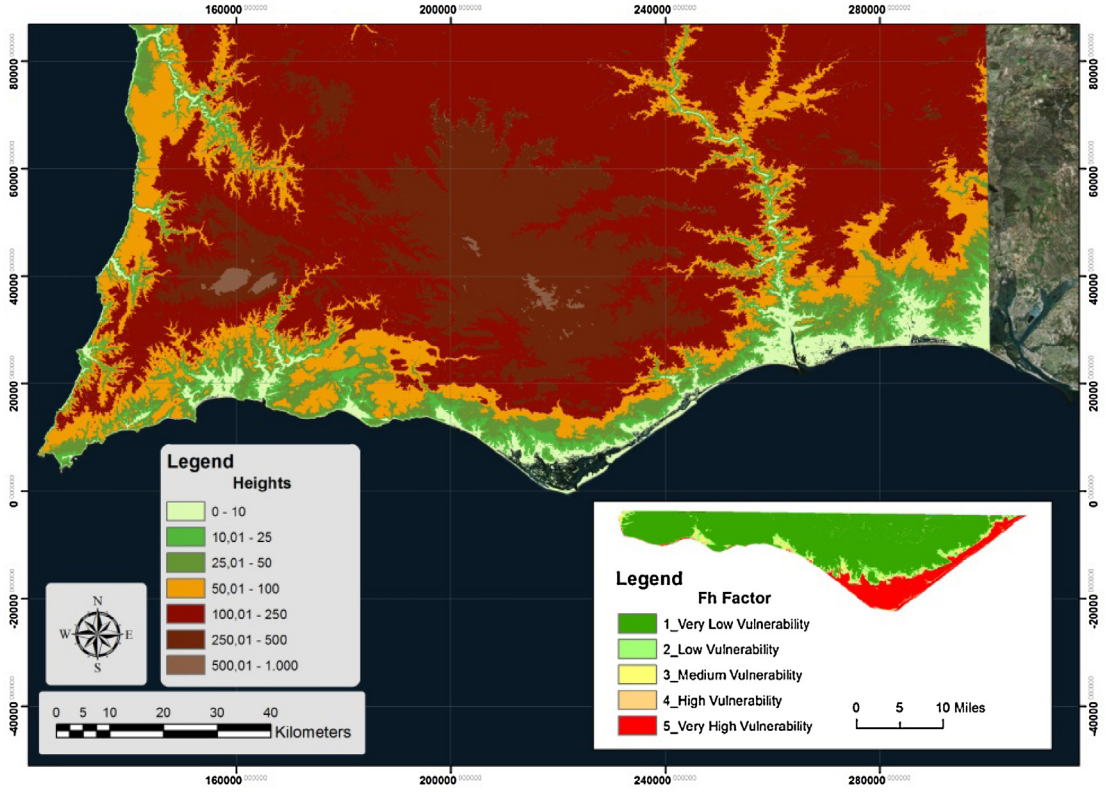

Fig. 5. Map of elevations (in meters) and reclassification according to vulnerability.

wavelength of wave fronts. Then, friction with the bottom progressively reduces velocity whereas wave crests continue practically unaffected. Eventually waves collapse and break (Barrera, 2005) are changing their morphology to a critical point where the distance to

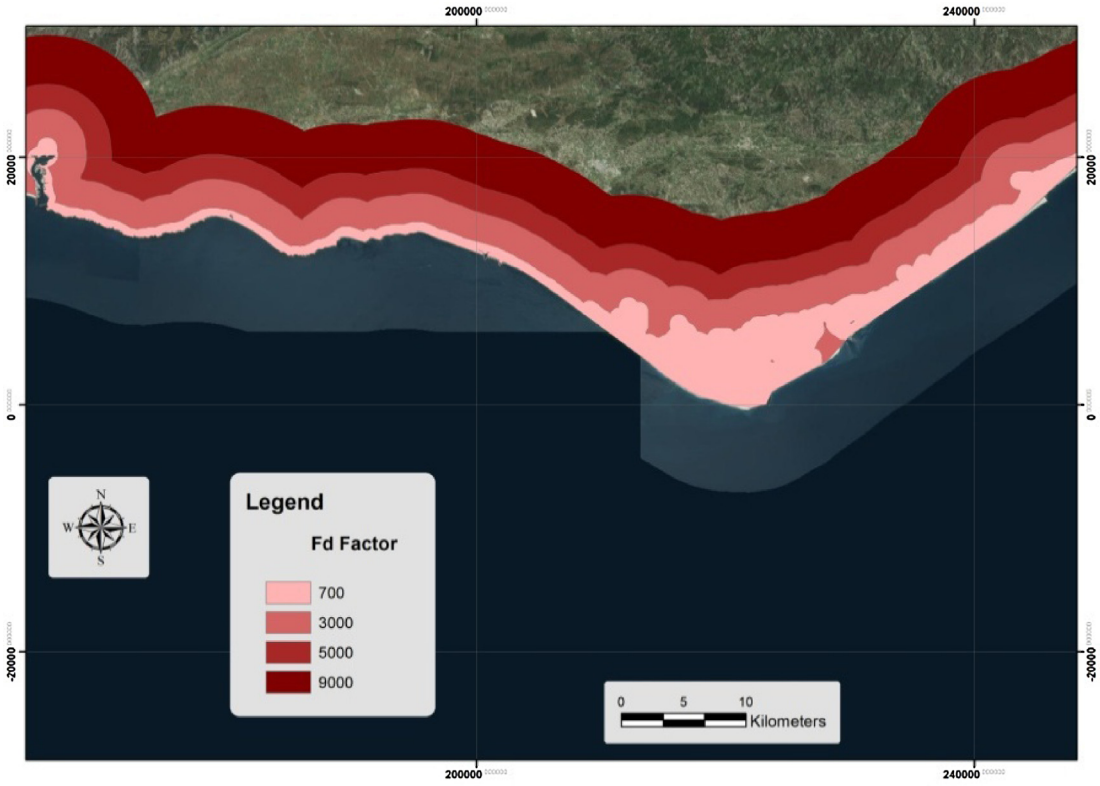

Fig. 6. Map of distances in meters.

the bottom is equal to half the wavelength of the wave fronts and brush with background destabilizes waves (water velocity in the ridge is higher than the bottom) and break (Barrera, 2005).

The bathymetry factor determines the ease of a greater or lesser marine ingression in the coastal sector, so that deeper progradation is higher than in shallow waters with less run up, where the depth is less than half the wavelength causing the swash of the waves.Since we have no data regarding the wave fronts, this factor provides information on the effect of waves on the beach and spits. Bathymetric maps take into account points and bathymetric curves supplied by the Hydrographic Service of the Portuguese Navy and the Oceanographic Institute of Spain, complemented with digital depth values in the channels of Ria Formosa. The resolution of the resulting bathymetry maps is 2 m per pixel.

The weight and reclassification was made taking into account that vulnerability will be high in shallow depths because it enhances the action of breaking waves. The intervals are: depths less than 1.5 m (value 5), 1.5–3 m (value 4) 3–10 m (value 3), 10–20 m (value 2) and >20 m (value 1) (Fig. 7). Water depths in the Algarve are relatively high, with values close to 200 m in front of the barrier island system of Faro, which is considered less vulnerable, while shallower waters in Portimão-Albufeira yield medium to high values of vulnerability.

2.1.7. Coastal factor/exchange rate for coastal waterfront (Fc)

The study of the evolution of the coastline and its morphological variations was carried out using overlay and proximity techniques implemented in GIS, by restoring the successive positions of coastline during the last 59 years (1956–2015). This analysis is based on the superposition of aerial photography of 1956 (American Flight- US Air Force coverage, green line in Fig. 8) at a resolution of 1 m, orthoimages of the 2005 Portuguese Orthophotography with a resolution of 50 × 50 cm (red line in Fig. 8) and finally the georeferenced aerial images ArcGIS Online Viewer 2015 (yellow line in Fig. 8). The position of successive coastlines have been digitized and analyzed by means of USGS—DSAS- extension for ArcGIS v10.3, in terms of rates of retreat or accretion (m/yr) during this period. High values of growth (progradation: coastline moves temporarily on coastal zone) mean high values of vulnerability, while negative rates indicate low values of vulnerability (coastline recedes and sea backwards inside), with the following intervals: < −2 m/year (value 5), −2 to −1 (value 4) −1 to 1 (value 3), 1–2 (value 2) and >2 (value 1). Overall, average values are presented (between −1 and 1 m/year) for the coastal retreat in all the Algarve coast (Fig. 8).

2.1.8. Swell factor. Average rate of significant wave (Fw)

The swell factor indicates the maximum values of mean significant wave (average wave heights considering the highest waves in the geodatabase considered) that affect the coastline of the Algarve. The historical average data have been obtained from the website of the State Ports of Spain (http://www.puertos.es/es-es/oceanografia/Paginas/portus.aspx) and different authors describe the conditions of maritime agitation and waves of some ports, such as Faro and Sines (Costa et al., 2001). We analyzed various types of networks: REDCOS (network of coastal buoys less than 100 m deep and near harbour facilities), WANA (from simulated time series of parameters of wind and swell data), SIMAR 44 (simulated data time series of atmospheric and oceanographic parameters), and REDEXT (network of deep water buoys, more than 200 m water depth). The studied time series includes the intervals 1958–2015 (52 years), 1983–2012 (29 years), and 1992–2015 (23 years). Data for each station are organized in files with the parameters to be considered (Fig. 9A–C).

Surf rates have been introduced into GIS in order to statistically process information and make interpolations. The rationale for taking the average significant wave instead the extreme was that it represents better the more probable wave states and it gives importance to representativeness as compared with the total rather than

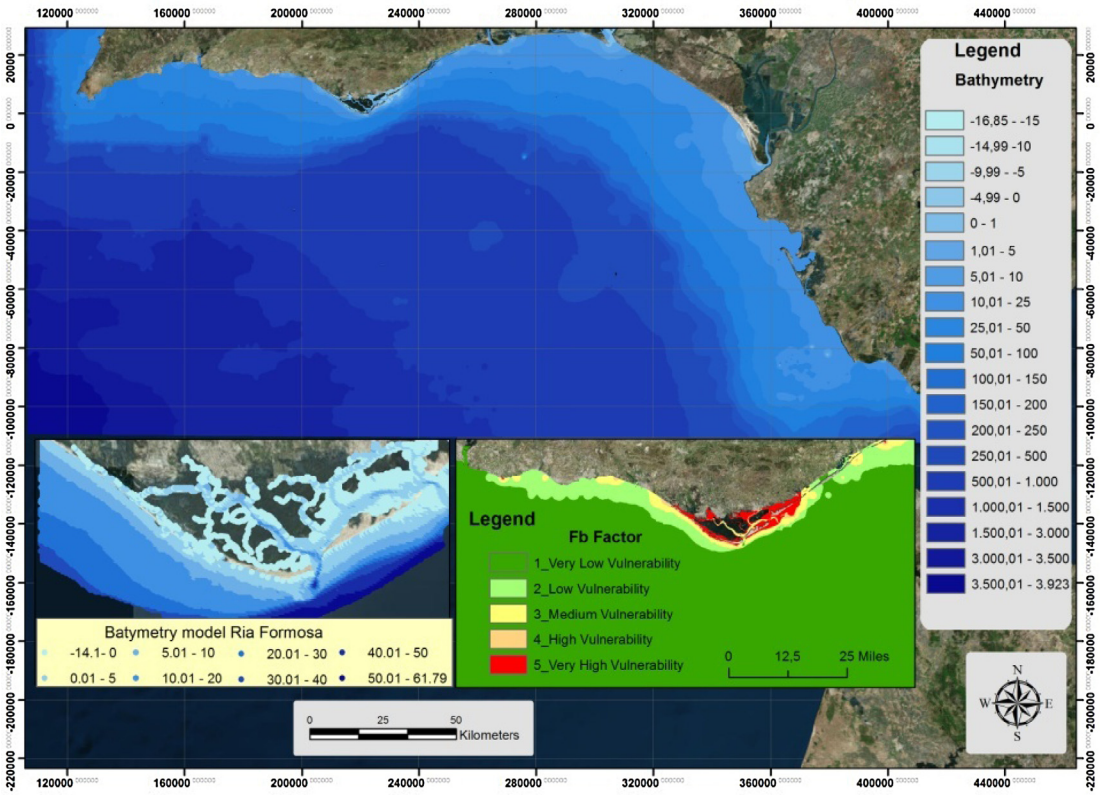

Fig. 7. Bathymetric maps (in meters) and reclassification of vulnerability.

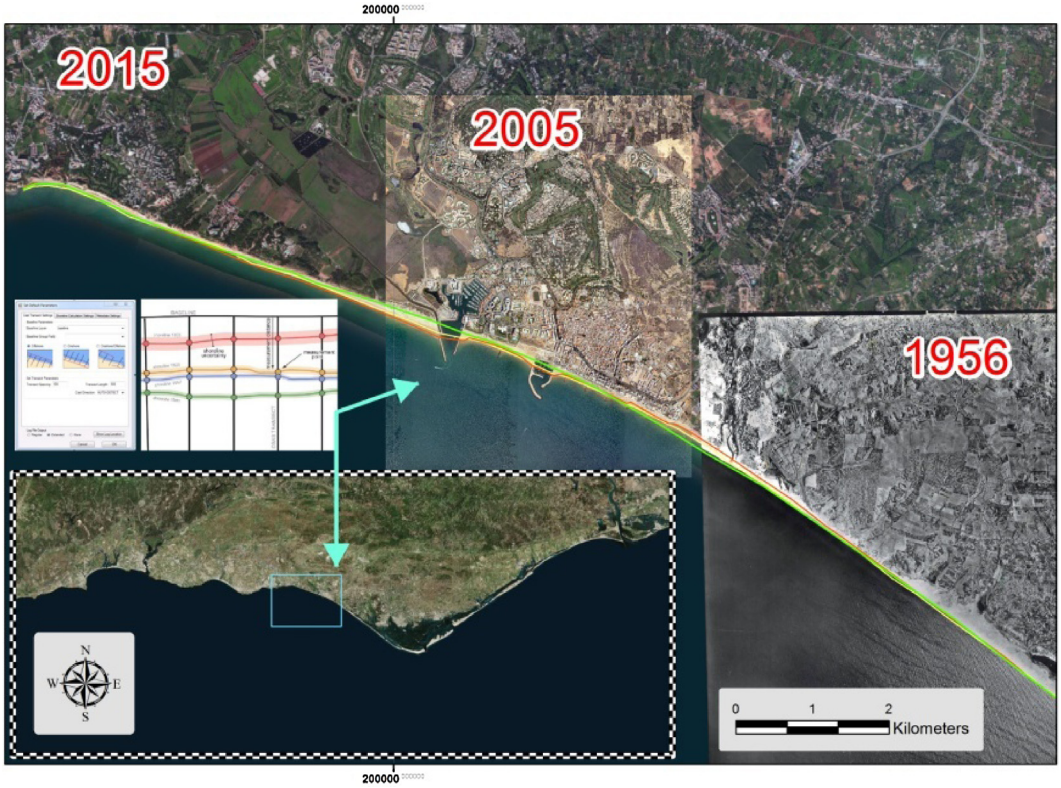

Fig. 8. Map of coastline variation analyzed with DSAS, for the 1956–2015 interval, superposition of aerial photography (green line 1956; red line (2005 and yellow line (2015). (For interpretation of the references to colour in this figure legend, the reader is referred to the web version of this article.)

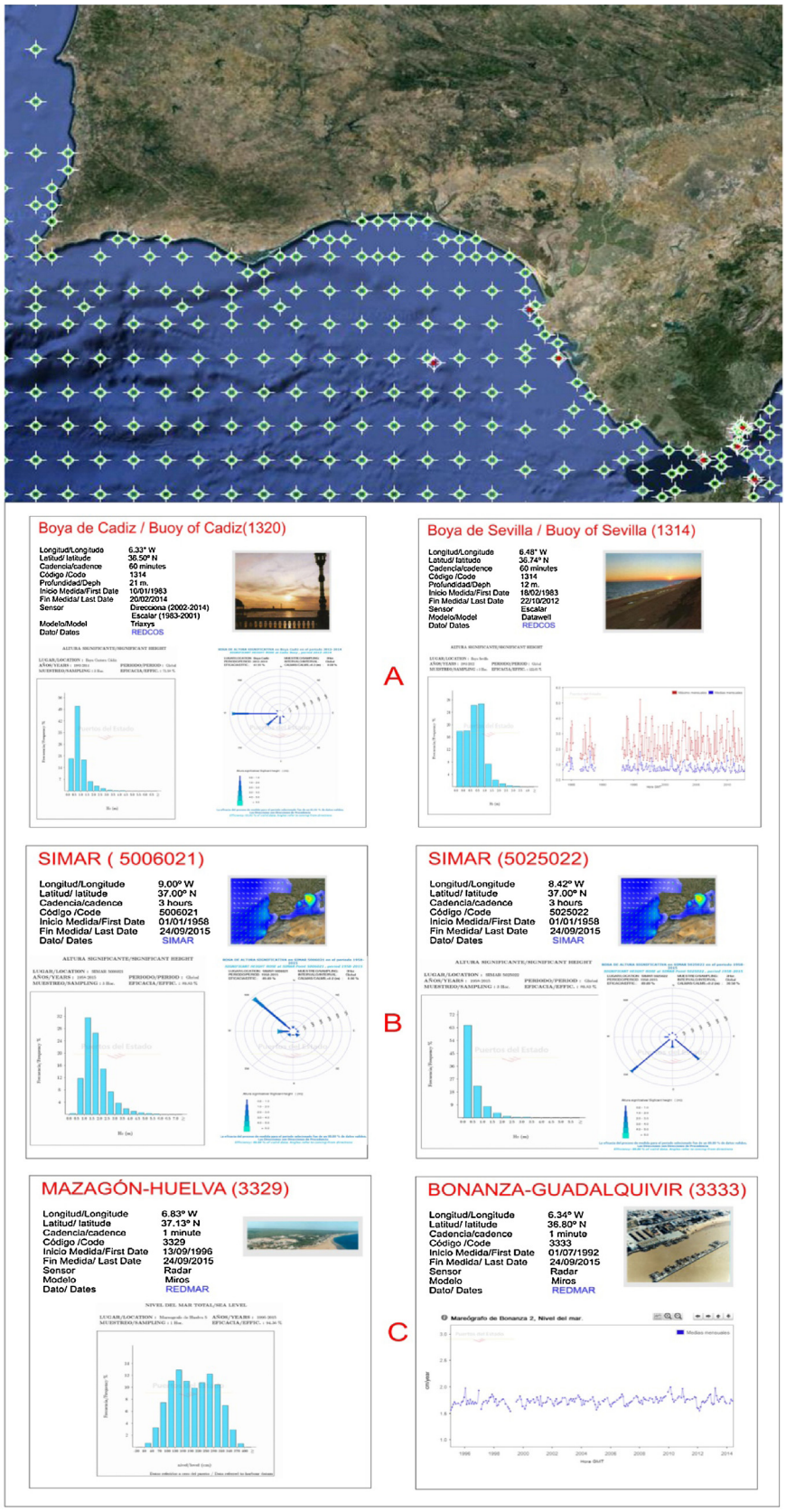

Fig. 9. Top: Historic data of stations with data buoys (red dots), simulated by models in points (green dots) and tide gauges (yellow dots). Bottom: examples of buoys files (A), SIMAR network (B) and REDEXT network (C). (For interpretation of the references to colour in this figure legend, the reader is referred to the web version of this article.)

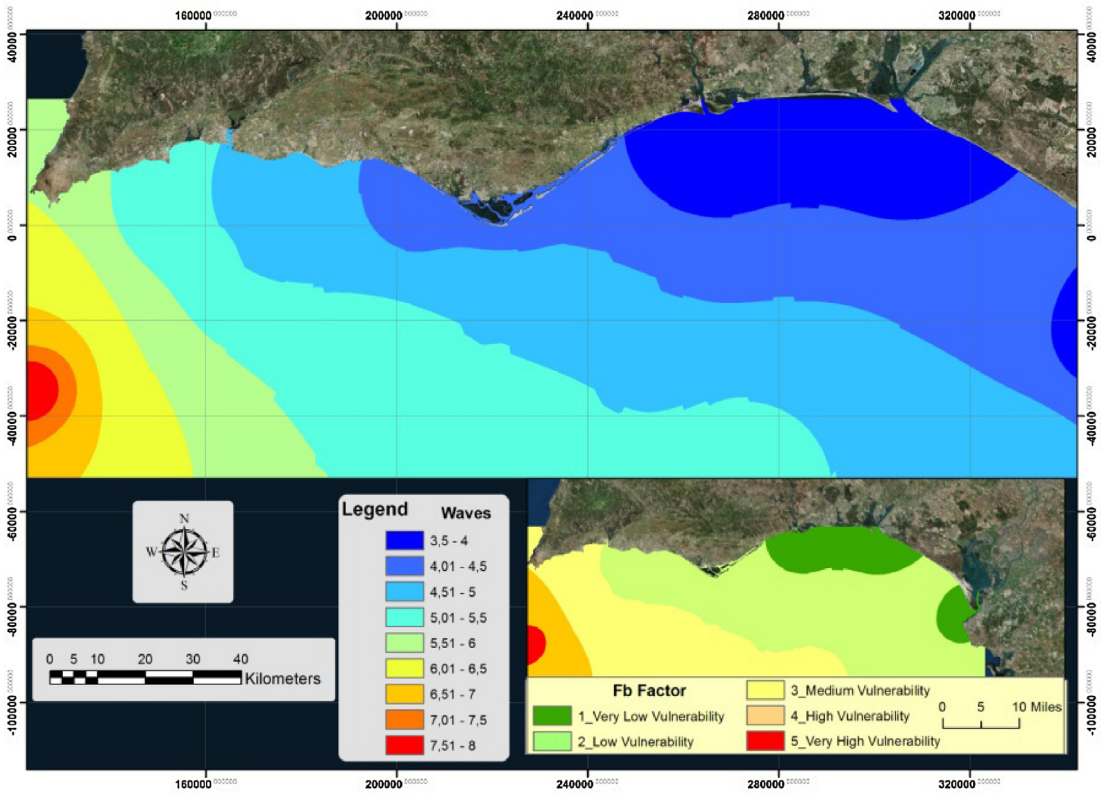

Fig. 10. Wave height factor map (in meters) for central Algarve.

focusing on sporadic episodes. We selected the highest values of the mean significant waves because our study is directed to the risk of flooding that would be statistically more probable (likely to occur), even if is less frequent. We took into account the longest temporal series for each measurement point (device). Vulnerability runs parallel to wave height, since higher waves mean a stronger effect on the coast, and assigned values are: 3.5–4 m (value 1), 4–5 m (value 2) 5–6 m (value 3) 6–7 m (value 4) and 7–8 m (value 5). According to the established parameters of wave height, vulnerability values for central Algarve coast would be high (between 3.5 and 5 m) (Fig. 10).

2.1.9. Sea level factor (Fsl)

This factor examines the relative sea level change using historical data of mean sea level (Borrego et al., 1995; Boski et al., 2008; Delgado et al., 2012; Sampath et al., 2014) collected by tide gauges along the nearby Spanish coast: Huelva, Cadiz and Tarifa (Fig. 9), which continuously evaluate and record the average level sea and tide gauge data of Portugal (Lagos and Cascais) records between 1908 and 1987 and 1882–1987 (Días and Taborda, 1988; Antunes and Taborda, 2009; Antunes, 2011). For this purpose we georeferenced and generated with ArcGIS the geodatabase of the closest tide gauges: gauges of Huelva 3.4 and 5 from 1996 to 2015 data, tide gauge Bonanza 2 at the mouth of the Guadalquivir river with data from 1992 to 2015, and Tarifa harbour tide gauge with data from 2009 to 2015. The network of stations is REDMAR (Fig. 9C).

Another source of data is the Permanent Service for Mean Sea Level—PSMSL-, located in Liverpool, UK. This organization collects, analyzes, interprets and publishes data related to the changes in the average global sea level, recorded by tide gauges. In addition to the existing network of tide gauges currently operative in various countries this Service incorporates data from tide gauges that worked in the past, adding long temporal series to the database. Data from the REDMAR network are incorporated periodically in international datacenters, one of which is PSMSL. As there are several representative series, we made a linear interpolation using ArcGIS v10.3 from the information provided by the gauges indicated above. For each time series, we obtained an average value of sea level oscillations which subsequently we divided by the number of years. This yields a rate for each tide gauge. The average rate of sea level rise for the study area, according to information provided by local tide gauge (1992–2015) ranges between 1.71 and 1.89 mm/year. Interpolating and reclassifying the interval in the central Algarve coast obtained values of the coast with the following weight interval: 1.29–1.34 (value 1), 1.341–1.46 (value 2), 1.461–1.58 (value 3), 1.581–1.70 (value 4) and 1.701–1.89 (value 5) (Fig. 11).

2.2. Extreme tidal range factor (Ftr)

The tidal range analyzes the difference in height between successive high and low tides. Depending on the geographical location and local conditions the tidal range can vary from a few centimeters to several meters. Coasts with tidal ranges below 2 m are considered microtidal (Masselink and Short, 1993). We analyzed the values of the nearest stations of the REDMAR network (Fig. 9) to know precisely fluctuations in the tidal range. Subsequently, we conducted a linear interpolation to obtain such data and hazard mapping as a measure for future prevention applied to coastal management. Because the ultimate goal of the study is to know the vulnerability and the risk of flooding, we have taken the maximum tidal ranges recorded for time series as representing highs, although in other cases the mean tidal ranges could be considered as representative. The tidal range obtained in the study area is about 2–4 m (Borrego et al., 2000), as expected in this mesotidal Atlantic coast (Fig. 12), with values between 120 cm (in the Strait of Gibraltar sector) and 420 cm. The reclassification of vulnerability values are: 120–180.1 cm (value 1), 180.2–240.1 (value 2), 240.2–300.1 (value 3) 300.2–360.1 (value 4) and 360.2–420 (value 5).

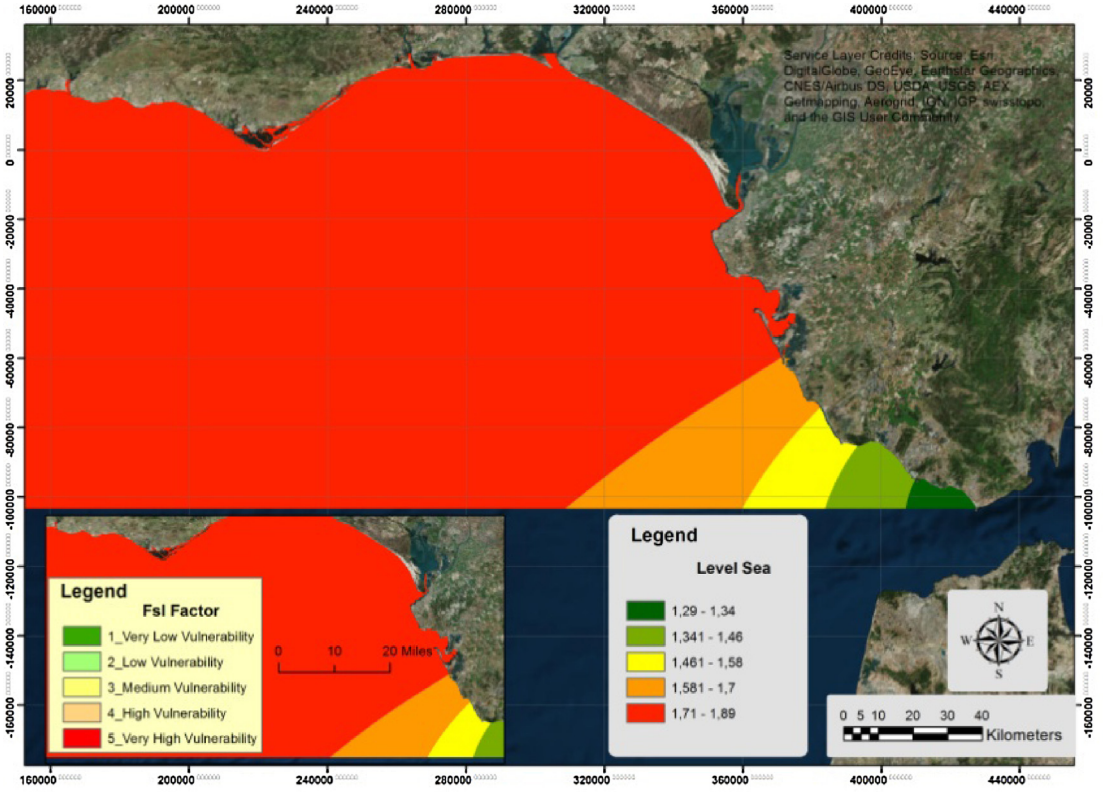

Fig. 11. Map of the average rise of sea level factor, expressed in millimeters, in Gulf of Cadiz.

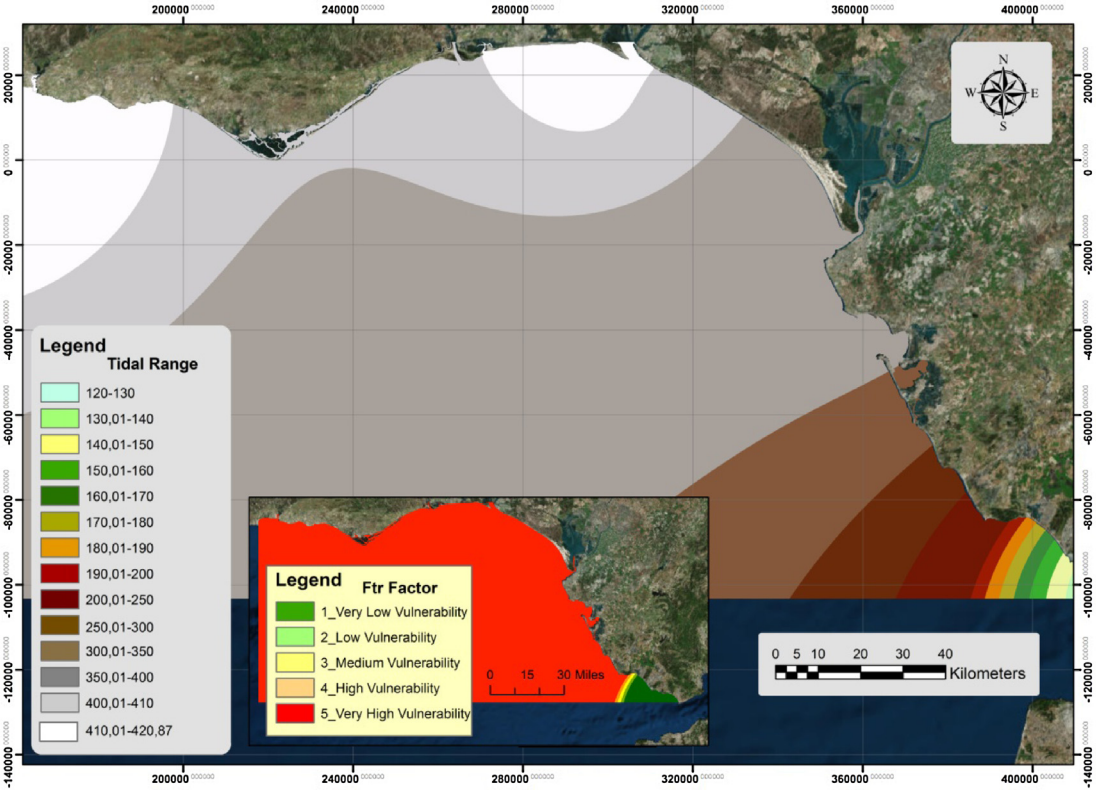

Fig. 12. Tidal range factor map (in centimeters) of Gulf of Cadiz.

2.3. Analysis of coastal flooding hazard

This analysis is based on the flood hazard index –FHI-, generating in this paper a novel contribution with is new index, which takes into consideration different scenarios of rise and fall of sea level from estimates, assuming that the rest of quantitative variables in the area (tidal range and waves) remain constant.

Recent studies (Church et al., 2013; Holgate et al., 2013; IPCC, 2014) based upon satellite altimeter data, calculated an annual increase in sea level rise of 3 mm/year between from 1993 and 2011. However, if these rates remain; the rise of sea level would reach values well above the estimated by other authors, influenced by thermal expansion and changes in salinity (Marcos and Tsimplis, 2008; Marcos et al., 2011). From the waves, tidal range and sea level parameters of studied in the analysis of vulnerability, we estimated the coastal flood hazard in different scenarios, considering that these are mean values for the past 25 years (mean of the time series of the available stations). The absolute rise in meters is calculated from minimum and maximum rise (mm/year) rates.

The study area is part of a zone of collision between the European and African plates, which can generate tsunamis. This is an area, where the depth of the basin acts as an aggravating factor (Lario et al., 2010, 2011). Also in surrounding areas there is evidence of records in Quaternary sedimentary series of extreme events of tsunami type, similar to the 1755 event (Lisbon earthquake) when sea level rose up to 8 m above the current level. That was the case of the event recorded in Conil town in the province of Cadiz, where the small fishing village of Conilete was completely destroyed and never reconstructed again (Luque et al., 2002). Other geological and historical records of lesser energetic storm events causing sudden rises of sea level are common in the area. These records, whether landforms or deposits, prove rises of sea level under storm conditions up to 2 m in elevation. The chronological sequence of occurrence of events, as expected, does not show cyclicity but the ages of these catastrophic events have been dated: 365 BC; 1680; 1804; 1860 and 1875 (Luque et al., 2001).

The Flood Risk Index –FHI- (Eq. (2)) considers three parameters that take into account the interaction between sea level rise and the physiographic features of the coastal strip, for different scenarios in our study area. The proposed scenarios are (Table 2):

$$vFHI = Fw \times Fsl \times Ftr_{(Xn)} \quad (2)$$

X_0 scenario (present): Represents the hazard of flooding based on data collected from tide gauges and buoys in the vicinity of the study area, based on data of the past 25 years.

X_1 scenario (100 years): Represents the hazard of flooding taking into account the data collected on stage X_0 calculated for the next 100 years.

X_2 scenario (500 years): Estimation of current sea level rise scenario for 500 years by extrapolating X_1 A stage.

X3 scenario (1000 years): Estimation of current sea level rise scenario for 1000 years based on predictions X_1 A stage.

X_4 scenario Extreme events: Storms (X_4) and tsunamis (X_4): probabilities of large events such as storms or tsunamis and their impact on the coast are added.

3. Results

3.1. Coastal vulnerability in the Portimão-Faro sector

From the "AVI" index calculated the vulnerability of the central sector of the Algarve, for a scenario $X_{3''}$ equivalent to sea level rise in 1000 years, from the factors that influence sea level rise. Particular attention was paid to the various sectors of the coastal strip. The higher the value of the AVI index, the higher vulnerability to rising sea level (Fig. 13).

Values of vulnerability are very high for the Faro sector, while in the area of Albufeira and Portimão the vulnerability index is medium-low. The distribution of areas of sea level rise is consistent with the risk analysis that will be explained below, although this is less intense and more conservative. High vulnerability also concentrates on sectors with high tourist population (Faro, Portimão, Olhos de Agua-W Quarteira, Pera . . ..). Note the high vulnerability of the International Faro airport, hotels and some nearby cities (Tavira, Olhão . . ..)

3.2. Risk of coastal flooding in Portimão-Faro sector

We have projected several future scenarios of sea level rise on a map based on the present (2015) orthophoto, where the different degrees of risk of coastal flooding in the coastal strip can be observed (Fig. 14) and the most densely populated areas are shown.

The map of hazards shows that the coastal strip of the more advanced waterfront (barrier islands of Faro) is the one experiencing the wider and greater penetration of sea water, whereas those areas unprotected by barrier islands (Albufeira) are less affected. Obviously, the topographically depressed areas, as is the case of river mouths are the most affected by a rising sea level, with more inland penetration of sea water (Portimão and Olhos de Agua). In some places with vital infrastructures, such as Faro International Airport, or touristic concentrations, such as Olhos de Agua and Portimão high flood hazard is observed. Along topographically high sectors such as Albufeira, flood bands are restricted to environments close to the present sea front: beaches, dune systems, for example (Fig. 15).

To assess the degree of risk exposure, several parameters are analyzed: surface, number of inhabitants in each municipality, population density, topographical height of the citie and distance from the town to the waterfront. From the map of land use of the European project Corine (Fig. 16, Table 3), the anthropic areas (neighborhoods, industrial areas, infrastructure. . ..) are determined and, using geospatial tools, the populated areas visible on the present aerial photography are delimited, obtaining the square kilometers of urbanized area. Algebra of layers allows easy calculation of the exposed population. Finally, linking the density of population of every zone to the flood risk in each sector, the exposed population for every scenario is calculated. This direct method is the most useful for authorities in charge of planning the risk of coastal flooding, because they can quickly update the thematic layers, as the process is a simple superposition. Other GIS techniques use indirect methods such as multivariate methods with spatial analyst Tools such as ISO cluster unsupervised classification, or also maximum likelihood classification. These indirect methods must first establish spectral signatures from digital image levels set by a technician using a basic supervised classification made by unsupervised classification extrapolated to the rest of the image. Its use is more costly and less flexible and slower than the direct method proposed in this paper.

The results of exposure to of flooding hazard in the central Algarve for different scenarios deduced from modeling of data obtained and potential urbanized areas affected, indicate that the coastal sector with wider urbanized area exposed to high hazard of sea flooding is 7.46 km^2 in surface, between Albufeira and Olhos de Agua, where a population density of 612.9 inhabitant/km^2 induces the highest risk of flooding for population in the central Algarve: 4572 people may be affected. In addition, Faro is the largest surface area exposed to the risk of flooding by sea level rise, with 8.784 km^2 and an exposed population of 2831 people. It is worth to note that some sectors of Faro, such as the airport area and parts

Table 2
Stages and parametric values of absolute and total estimated rise in sea level as the present study.

Scenario Factor	Fw		Fsl		Ftr		Total	
	Min	Max	Min	Max	Min	Max	Min	Max
Present Scenario—X_0	3.5	5	0.042	0.047	4.0	4.2	**7.54**	**9.24**
100 years Scenario—X_1	3.5	5	0.12	0.14	4.0	4.2	**7.62**	**9.34**
500 years Scenario—X_2	3.5	5	0.63	0.70	4.0	4.2	**8.13**	**9.90**
1000 years Scenario—X_3	3.5	5	1.26	1.40	4.0	4.2	**8.76**	**10.60**
Storm Scenario—X_4	3.5	5	2 m		4.0	4.2	**9.50**	**11.20**
Tsunami Scenario—X_5	3.5	5	8 m		4.0	4.2	**15.50**	**17.20**

Bold represents the final values.

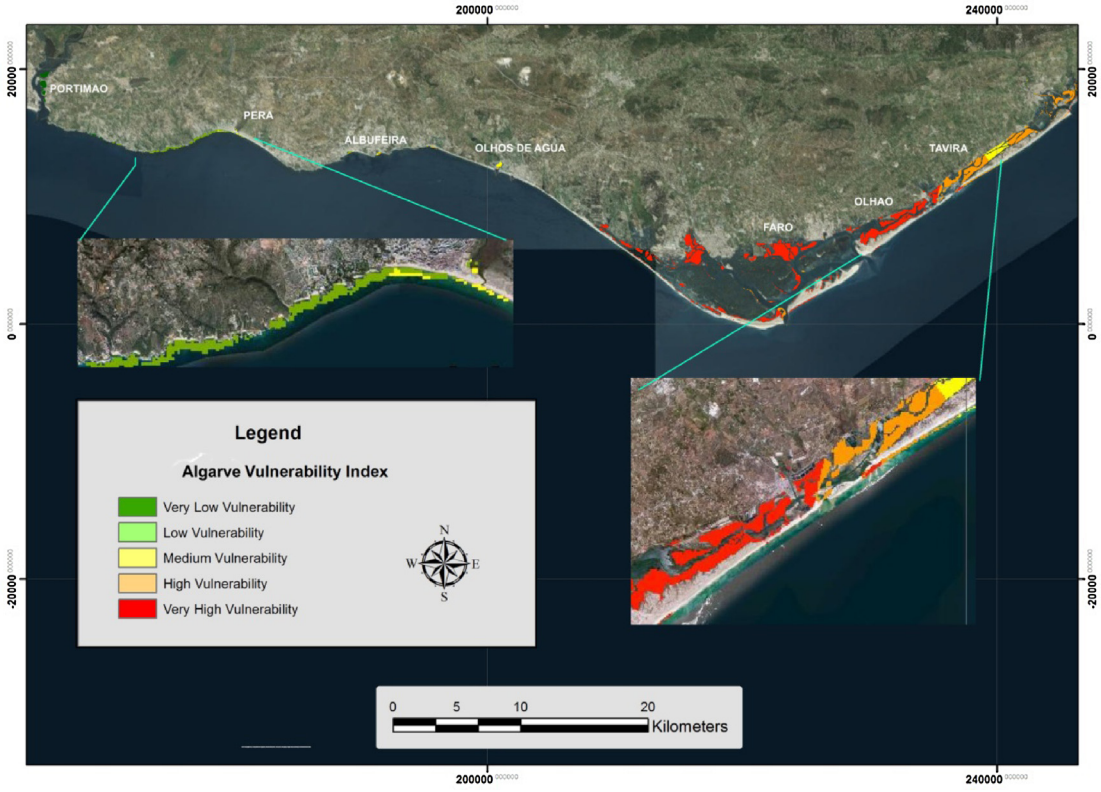

Fig. 13. Map of the Coastal Vulnerability central Algarve as the—AVI- index.

Table 3
Parameters for the calculation of exposure to risk of flooding.

Municipality Factor	Area (Km^2)	Inha-bitants.	Density of population (Inh/Km^2)	City elevation above sea level (m)	Distance to coastline (Km)	Urbanized area exposed (Km^2)	Inha-bitants exposed
Portimao	182.06	55614	305.47	2	3	5.52	1686
Pera	9.15	4867	531.9	7	0	2.42	1287
Albufeira-Olhos de Agua	140.91	38966	612.9	8	0–2	7.46	4572
Quarteira	37.78	16131	427	3	0	0.39	166
Faro	202.57	64560	318	12	0	8.84	2831
Olhao	130.90	42272	322.9	8	0	6.52	2105
Tavira	764.4	69824	91.34	28	0	3.88	354

of the old town near the harbour, would be flooded in a temporally near scenario (scenario X_1)

4. Conclusions

The results provide valuable information on the degree of vulnerability and the risk profile of the Algarve in the event of a potential rise in sea level whether it is generated by a progressive rise or during extreme events.

The vulnerability has been calculated from the Algarve vulnerability index —AVI. The maps of vulnerability and risk highlight the high risk of flooding posed by any rise, however small, in the Algarve coast. The urbanized area affected by flood risk is about 35 km^2, but the figure is higher if crop and not populated areas are incorporated. The population subjected to flooding risk in central Algarve coastal areas amount to some 13,000 people, with a higher exposure in the sectors of Albufeira, Olhos de Agua and Faro.

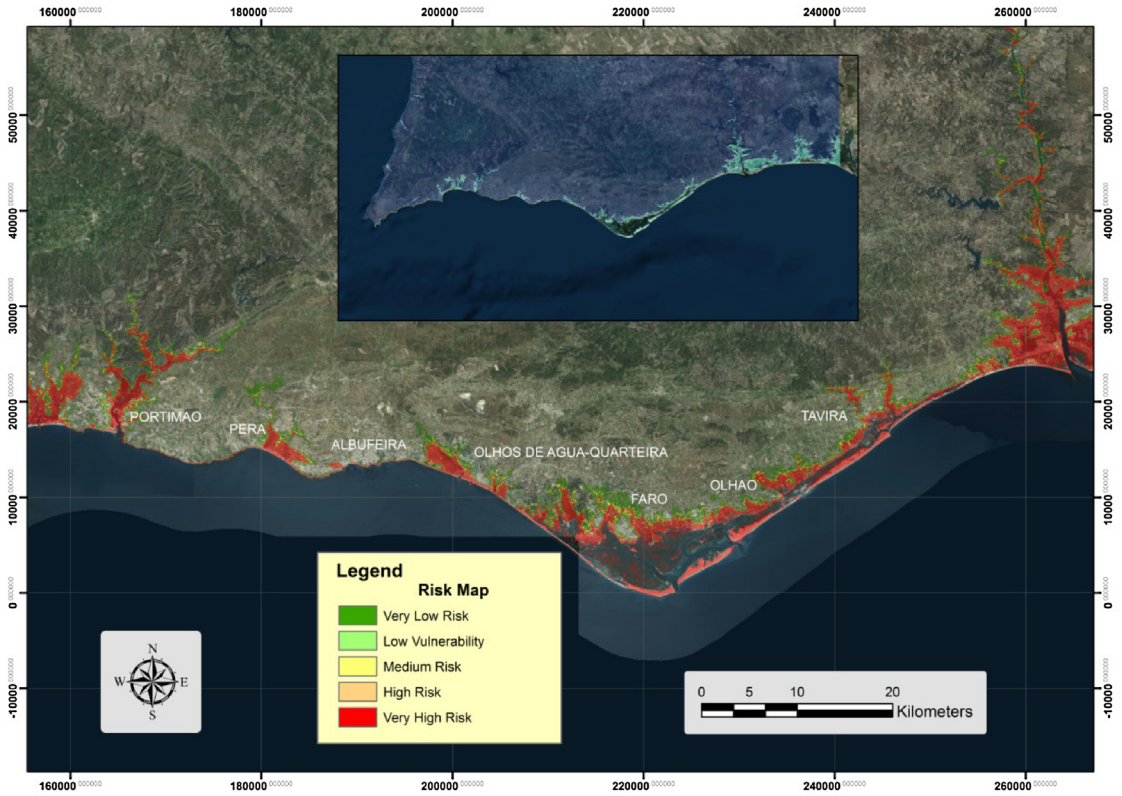

Fig. 14. Flood Hazard Map for the central Algarve coastline under—AVI- index for 1000 years Scenario: X_3.

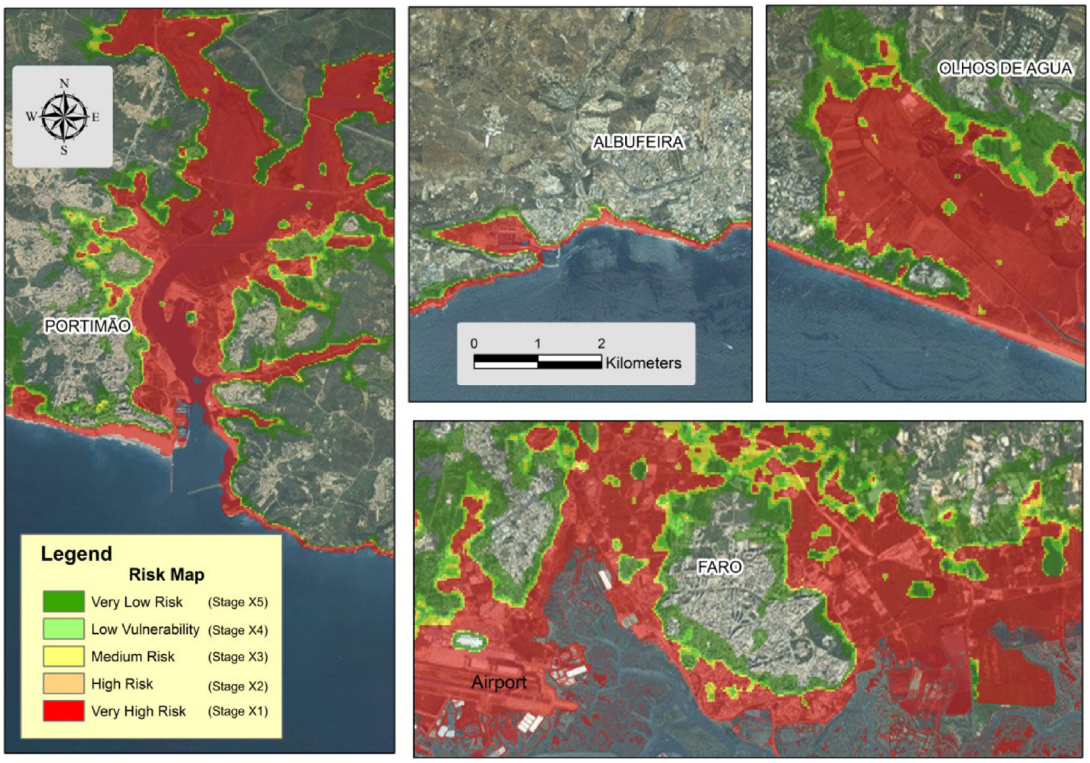

Fig. 15. Detail of the flood hazard for some localities on the coastal strip of central Algarve for 1000 years Scenario: X_3.

The short time series available from tide gauges and buoys, coupled with the continuous change of estimates of trends for the century make the subject of current sea level rise in a most controversial one. The broad spectrum of future prospects, coupled with the uncertainty of the past (the oldest measurements from tide gauges date from 1883) leave the sedimentary record as one of

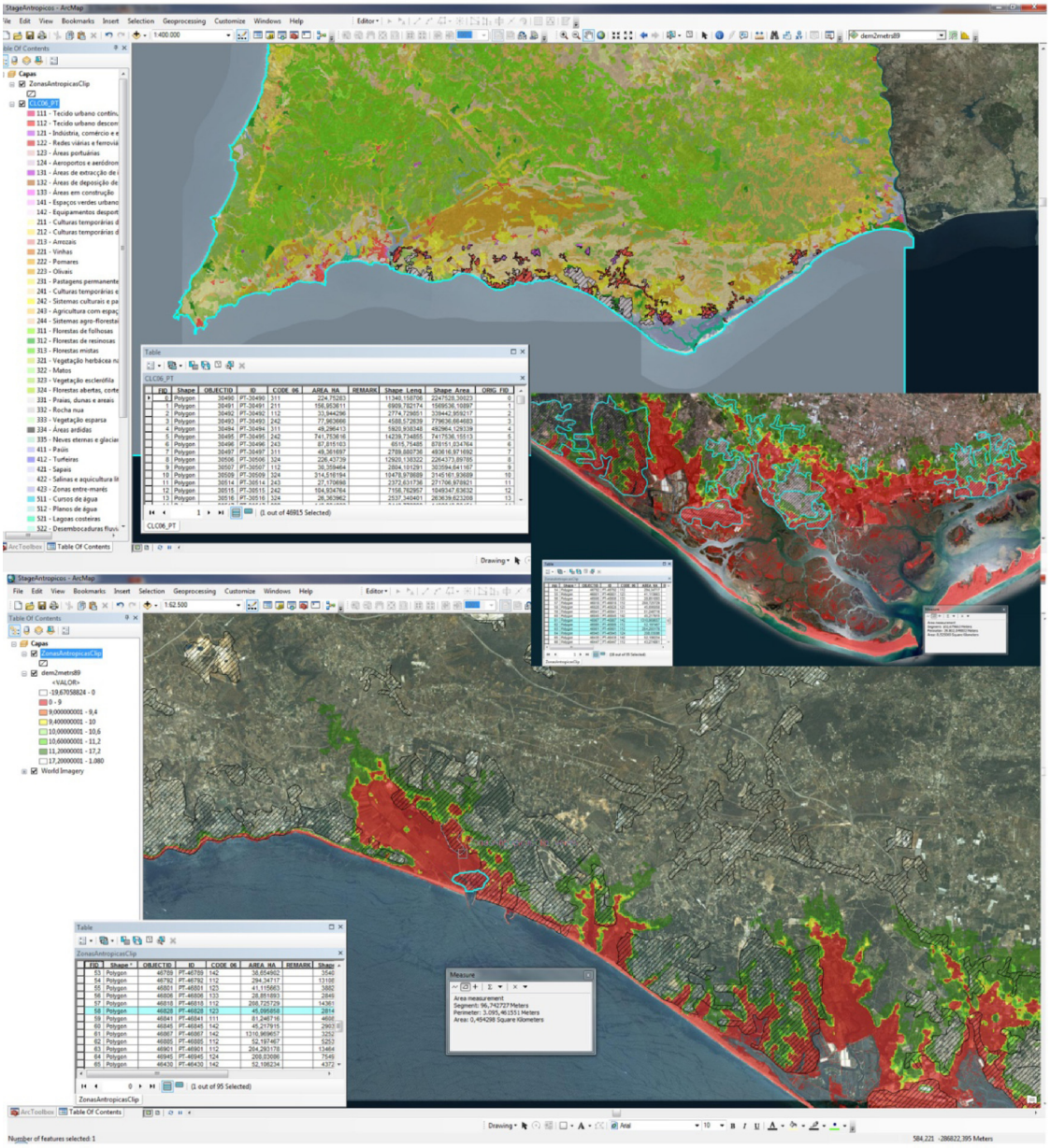

Fig. 16. Top: CORINE map, showing the different land uses and associated geodatabase. Bottom: example of calculation at risk of flooding from built-up areas (polygons with black stripe) on the flooded areas for different stages (map legend 15) in the area of Olhos de Agua.

the few witnesses of the change in sea level, which in turn is rather unprecise both temporally and spatially.

The methodology used here is self-validating because the affected areas calculated by the method of vulnerability (based on empirical methods of parameters of the study area) match with those obtained by the method of risk (based on deterministic methods, using temporal trend scenarios). Many forecasts on the quantification of the current sea level rise globally do not consider the swell factor and tidal range, thus invalidating to some extent a direct transposition of these values over a specific area. For this reason, local studies, such as the present, which address and evaluate the risks of flooding under the worst-case rising scenario simulated, are much more reliable.

Finally this mapping is a preventive measure to minimize the risk in this coast, with large developments and resorts, and visited by herds of tourists from all around the world. Using this tool, management actors can delimitate the sectors in need of structural measures aimed to minimize short- and long- term impacts of sea level rise caused by natural tendency or by extreme events. The Algarve coast is a highly vulnerable area owing to the characteristics of the physical environment and a high risk of flooding because of its geographical position.

Acknowledgment

Ministry of Economy and Competitiveness: BTE, CGL2012-33430/BTE and CGL2012-37581/BTE.

References

Andrade, C., Freitas, M.C., Moreno, J., Craveiro, S.C., 2004. Stratigraphical evidence of Late Holocene barrier breaching and extreme storms in lagoonal sediments of Ria Formosa Algarve, Portugal. Mar. Geol. 210 (1–4), 339–362.

Antunes, C., Taborda, R., 2009. Sea level at Cascais Tide Gauge: data, analysis and results. J. Coast. Res. 56, 218–222 pp.

Antunes, C., 2011. Monitoring sea level change at Cascais tide gauge. J. Coast. Res. 64, 870–874 pp.
Barrera, N., 2005. Influencia del rebase del oleaje en playas sobre lagunas costeras. El caso de la laguna de la Magarola. Universidad Politécnica de Cataluña—UPC-. http://upcommons.upc.edu/pfc/bitstream/2099.1/3386/5/40860-5.pdf (acceso: 5/10/15).
Bindoff, N.L., Willebrand, J., Artale, V., Cazenave, A., Gregory, J., Gulev, S., Hanawa, K., Le Quéré, C., Levitus, S., Nojiri, Y., Shum, C.K., Talley, L.D., Unnikrishnan, A., 2007. Observations: oceanic climate change and sea level. In: Solomon, S., Qin, D., Manning, M., Chen, Z., Marquis, M., Averyt, K.B., Tignor, M., Miller, H.L. (Eds.), Climate Change 2007: The Physical Science Basis. Contribution of Working Group I to the Fourth Assessment Report of the Intergovernmental Panel on Climate Change. Cambridge University Press Cambridge, United Kingdom and New York, NY, USA.
Borrego, J., Morales, J.A., Pendón, J.G., 1995. Holocene estuarine faciesalong the mesotidal coast of Huelva, southwestern Spain. In: Fleming, B.W., Bartholomä, A. (Eds.), Tidal Signatures in Ancient and Modern Environments, vol. 24. Spec. Publs, Int. Assoc. Sediment, pp. 151–170.
Borrego, J., Morales, J.A., Gil, N., 2000. Evolución sedimentaria reciente de la desembocadura de la ría de Huelva (SO España). Rev. Soc. Geol. Esp. 13 (3–4), 405–416.
Boski, T., Camacho, S., Moura, D., Fletcher, W., Wilamowski, A., Veiga-Pires, C., Correia, V., Loureiro, C., Santana, P., 2008. Chronology of post-glacial sea-level rise in two estuaries of the Algarve coast S. Portugal. Estuar. Coast. Shelf Sci. 77, 230–244.
Church, J.A., White, N.J., 2011. Sea-Level rise from the late 19th to the early 21st century. Surv. Geophys. 32, http://dx.doi.org/10.1007/s10712-011-9119-1, 585–602 pp.
Church, J.A., Clark, P.U., Cazenave, A., Gregory, J.M., Jevrejeva, S., Levermann, A., Merrifield, M.A., Milne, G.A., Nerem, R.S., Nunn, P.D., Payne, A.J., Pfeffer, W.T., Stammer, D., Unnikrishnan, A.S., 2013. Sea level change. In: Stocker, T.F., Qin, D., Plattner, G.-K., Tignor, M., Allen, S.K., Boschung, J., Nauels, A., Xia, Y., Bex, V., Midgley, P.M. (Eds.), Climate Change 2013: The Physical Science Basis. Contribution of Working Group I to the Fifth Assessment Report of the Intergovernmental Panel on Climate Change. Cambridge University Press Cambridge, United Kingdom and New York, NY, USA.
Conde, E., 2015. The race for the arctic: international law issues considering climate change. In: Simposio International Symposium: El Ártico: Oportunidades Y Riesgos Derivados Del Cambio Climático, Fundación Ramón Areces Nov.12, Fundación Ramón Areces, Madrid, Ref. DER2012-36026.
Costa, M., Silva, R., Vitorino, J., 2001. Contribução para o estudo do clima de agitação marítima na costa portuguesa. In: II Jornadas De Engenharia Costeira E Portuaria, Aveiro, 20 pp.
Días, J.M.A., Taborda, R.P.M., 1988. Evolução recenté do nível médio do mar em Portugal. An. Inst. Hidrogr. 9, 83–97 pp.
DOUE 60, 2007. Assessment and management of flood risks entered into force on 26 November 2007. (Directive 2007/60/EC) http://ec.europa.eu/environment/water/flood_risk/index.htm (access: 15/11/15).
Delgado, J., Boski, T., Nieto, J.M., Pereira, L., Moura, D., Gomes, A., Sousa, C., García-Tenorio, R., 2012. Sea-level rise and anthropogenic activities recorded in the late Pleistocene/Holocene sedimentary infill of the Guadiana Estuary (SW Iberia). Quat. Sci. Rev. 33, 121–141, http://dx.doi.org/10.1016/j.quascirev.2011.12.002.
Grinsted, A., Moore, J.C., Jevrejeva, S., 2010. Reconstructing sea level from paleo and projected temperatures 200–2100 AD. Clim. Dyn. 34, 461–472.
Hammar-Klose, E., Thieler, E.R., 2001. Coastal Vulnerability to Sea-Level Rise: A Preliminary Database for the U.S. Atlantic. Pacific and Gulf of Mexico Coasts U.S. Geological Survey Digital Data Series, pp. 68, http://pubs.usgs.gov/dds/dds68/ (access: 22/11/15).
Holgate, S.J., Matthews, A., Woodworth, P.L., Rickards, L.J., Tamisiea, M.E., Bradshaw, E., Foden, P.R., Gordon, K.M., Jevrejeva, S., Pugh, J., 2013. New data systems and products at the permanent service for mean sea level. J. Coast. Res. 29 (3), 493–504, http://dx.doi.org/10.2112/JCOASTRES-D-12-00175.1.
IPCC, 2014. Climate change 2014. In: Core Writing Team, Pachauri, R.K., Meyer, L.A. (Eds.), Synthesis Report. Contribution of Working Groups I, II and III to the Fifth Assessment Report of the Intergovernmental Panel on Climate Change. IPCC, Geneva, Switzerland, 151 pp.
Jonkman, S.N., Kelman, I., 2005. Deaths during the 1953 North Sea storm surge. http://www.rigsystems.co.uk/members/content/documents/1cd05-6547a.pdf (access: 22/11/15).
Katsman, C.A.G., Oldenborgh, J.V., 2011. Exploring high-end scenarios for local sea level rise to develop flood protection strategies for a low-lying delta—the Netherlands as an example. Clim. Dyn. 109, 617–645.
Kopp, R.E., Simons, F.J., Mitrovica, J.X., Maloof, A.C., Oppenheimer, M., 2009. Probabilistic assessment of sea level during the last interglacial stage. Nature 462, 863–868.
Kulkarni, A.T., Mohanty, J., Rao, T.I., Mohan, B.K., 2014. A web based integrated flood assessment modeling tool for coastal urban watersheds. Comput. Geosci. 64, 7–14 pp.
Kurt, L., Antonioni, F., Purcell, A., Silenzi, S., 2004. Sea level change along the Italian coast for the past 10,000 yr. Quat. Sci. Rev. 23, 1567–1598 pp.
Kurt, L., Antonioli, F., Anzidei, M., Ferranti, L., Leoni, G., Scicchitano, G., Silenzi, S., 2011. Sea level change along the italian coast during the Holocene and projections for the future. Quat. Int. 232, 250–257 pp.
Lario, J., Luque, L., Zazo, C., Goy, J.L., Spencer, C., Cabero, A., Bardají, T., Borja, F., Dabrio, C.J., Civis, C., González-Delgado, J.A., Borja, C., Alonso-Azcárate, J., 2010. Tsunami vs. storm surge deposits: a review of the sedimentological and geomorphological record of Extreme Waves Events (EWE) during the Holocene in the Gulf of Cadiz, Spain. Z. Geomorphol. 54 (Suppl. 3), 231–235 pp.
Lario, J., Zazo, C., Goy, J.L., Silva, P.G., Bardají, T., Cabero, A., Dabrio, C.J., 2011. Holocene paleotsunami catalogue of SW iberia. Revista Cuaternario Internacional 242, 196–200.
Luque, L., Lario, J., Zazo, C., Goy, J.L., Dabrio, C.J., Silva, P.G., 2001. Tsunami deposits as paleoseismic indicators: examples from the Spanish coast. Acta Geol. Hisp. 36 (3–4), 197–211.
Luque, L., Lario, J., Civis, J., Silva, P.G., Zazo, C., Go, y.J.L, Dabrio, J., 2002. Sedimentary record of a tsunami during Roman times, Bay of Cadiz, Spain. J. Quat. Sci. 17 (5–6), 623–631.
Manuppella, G., Ramalho, M., Antunes, M.T., Pais, J., 2007. Carta Geológica de Portugal, Folha 53-A. Faro. I nstituto Nacional de Engenharia tecnología e Innovação, 40 pp.
Marcos, M., Tsimplis, M.N., 2008. Coastal sea level trends in Southern Europe. Geophys. J. Int. 175 (1), 70–82.
Marcos, M., Jordà, G., Gomis, D., Pérez, B., 2011. Changes in storm surges in southern Europe from a regional model under climate change scenarios. Glob. Planet. Change 77 (3–4), 116–128, http://dx.doi.org/10.1016/j.gloplacha.2011.04.002.
Masselink, G., Short, A.D., 1993. The effect of tidal range on beach morphodynamics and morphology: a conceptual beach model». J. Coast. Res. 9 (3), 785–800.
Meehl, G.A., 2007. Global climate projections. In: Solomon, S., Qin, D., Manning, M., Chen, Z., Marquis, M., Averyt, K.B., Tignor, M., Miller, H.L. (Eds.), Climate Change 2007: The Physical Science Basis. Contribution of Working Group I to the Fourth Assessment Report of the Intergovernmental Panel on Climate Change. Cambridge University Press Cambridge, United Kingdom and New York, NY, USA, pp. 755–828.
Moura, D., Boski, T., 1999. Unidades litoestratigráficas do pliocénico e plistocénico no algarve, vol. 86. Com. Inst. Geol. E Mineiro, Lisboa, 85–106 pp.
Moura, D., Albardeiro, L., Veiga-Pires, C., Boski, T., Tigano, E., 2006. Morphological features and processes in the central Algarve rocky coast (South Portugal). Geomorphology 81, 345–360 pp.
Moura, D., Boski, T., Viegas, J., Veiga-Pires, C., 2009. Fronteira Pliocénico-Plistocénico: estudo de caso nas formações detríticas do Algarve, VII Reunião do Quaternário Ibérico, Ed CIMA 46–50.
Nicholls, R., Mimura, N., 1998. Regional issues raised by sea-level rise and their policy implications. Clim. Res. 11, 5–18.
Ojeda, J., Álvarez, J.I., Martín, D., Fraile, P., 2009. El uso de las TIG para el cálculo del índice de vulnerabilidad costera (CVI) ante una potencial subida del nivel del mar en la costa andaluza, vol. 9. Revista internacional de ciencia y tecnología de la información geográfica, España, 83–100 pp.
Pais, J., Cunha, P.P., Pereira, D., Legoinha, P., Dias, R., Moura, D., Silveira, A.B., Kullberg, J.C., González-Delgado, J.A., 2012. The Paleogene and Neogene of Western Iberia (Portugal). A Cenozoic Record in the European Atlantic Domain. Springer-Verlag, http://dx.doi.org/10.1007/978-3-642-22401-0, 158 p.
Pereira, R., Cabral, J., 2002. Interpretation of recent structures in an area of cryptokarst evolution-meotectonic versus subsidence genesis. Geodin. Acta 15, 233–248 pp.
Pfeffer, W.T., Harper, J.T., O'Neel, S., 2008. Kinematic constraints on glacier contributions to 21st-century sea-level rise. Science 321, 1340–1343.
Pilkey, O.H., Davis, T.W., 1987. An analysis of coastal recession models, North Carolina coast. In: Nummedal, D., Pilkey, O.H., Howard, J.D. (Eds.), Sea-level Fluctuation and Coastal Evolution, vol. 41. SEPM (Society for Sedimentary Geology) Special Publications, Tulsa, Okla, 59–68 pp.
Rahmstorf, S., 2007. A semi-empirical approach to projecting future sea-level rise. Science 315, 368–370.
Rodrigues, B.A., Matias, A., Ferreira, O., 2012. Overwash hazard assessment. Geol. Acta 10 (4), 427–439 pp.
Sampath, D.M.R., Boski, T., Loureiro, C., Sousa, C., 2014. Modelling of estuarine response to sea-level rise during the Holocene: application to the Guadiana Estuary—SW Iberia. geomorphology na estuary—SW Iberia. Geomorphology 232, 47–64.
Tooley, M., Jelgersma, S., 1992. Impacts of Sea-Level Rise on European Coastal Lowlands. Blackwell, P. 267 pp.
Vellinga, M., Wood, R., 2008. Impacts of thermohaline circulation shutdown in the twenty-first century. Clim. Change 91, 43–63.
Vermeer, M., Rahmstorf, S., 2009. Global sea level linked to global temperature. Proc. Natl. Acad. Sci. U. S. A. 106, 21527–21532.
Zazo, C., 2015. Explorando las costas de un pasado reciente: Los cambios del nivel del mar y climáticos. In: Discurso de Recepción de Académico Numerario. Real Academia de Ciencias Exactas Físicas y Naturales, Realigraf, 76 pp.